

Test of J -matrix inverse scattering potentials on electromagnetic reactions of few-nucleon systems

Nir Barnea

The Racah Institute of Physics, The Hebrew University, 91904 Jerusalem, Israel

Winfried Leidemann* and Giuseppina Orlandini*

*Department of Physics, The George Washington University, Washington DC 20052, USA and**Istituto Nazionale di Fisica Nucleare, Gruppo Collegato di Trento*

(Received 6 July 2006; published 22 September 2006)

The J -matrix inverse scattering nucleon-nucleon potentials (JISP), describing both two-nucleon data and bound and resonant states of light nuclei to high accuracy, are tested on the total photoabsorption cross sections of ^2H , ^3H , and $^3,4\text{He}$. The calculations in the three- and four-body systems are carried out via the Lorentz integral transform method and the hyperspherical harmonics (HH) technique. To this end the HH formalism has been adapted to accommodate nonlocal potentials. The cross sections calculated with the JISP are compared to those obtained with more traditional realistic interactions, which include two- and three-nucleon forces. Although the results of the two kinds of potential models do not differ significantly at lower energies, beyond the resonance peak they show fairly large discrepancies, which increase with the nuclear mass. We argue that these discrepancies may be due to a probably incorrect long-range behavior of the JISP, because the one pion exchange is not manifestly implemented there.

DOI: [10.1103/PhysRevC.74.034003](https://doi.org/10.1103/PhysRevC.74.034003)

PACS number(s): 21.45.+v, 21.30.-x, 25.20.Dc, 27.10.+h

I. INTRODUCTION

In the past few years the possibility to perform very accurate calculations in few-nucleon systems has stimulated a new attitude in studying the nature and form of the nuclear force. Differently from what was common in the past, nowadays potential models are tested not only on the increasingly accurate nucleon-nucleon (NN) data and triton binding energy but also on bound and resonant states of more complex systems.

The modern debate on nuclear forces focuses on potential models that can schematically be grouped into three different categories. Category A includes the most traditional potentials. Their two-body parts either are based on meson exchange models [1–3] or are largely phenomenological [4,5]. However, all of them include the essential one-pion exchange term at long range and reproduce the NN -scattering data with very high accuracy. However, when tested on $A \geq 3$ nuclei, they show nonnegligible underbinding. Three-body forces have been introduced to fit the $A = 3$ binding energy and more recently also to describe energies of bound and low-lying resonant states of p -shell nuclei [6–9].

Category B includes the effective field theory (EFT) potentials [10], which have a stronger connection to quantum chromodynamics (QCD). They imply consistent two-, three-, or more-body terms. The number of these terms and of the associated parameters, as well as the accuracy in reproducing data, increase significantly with the order of the expansions. The common feature of potentials belonging to categories A and B is the presence of three-body operators. These require very intense computational efforts when used in many-body systems.

Category C includes potentials that, although describing NN -scattering data with high accuracy make use of the remaining off-shell freedom to reproduce few-body ground-state energies and low-lying resonances, avoiding the necessity of three-body operators [11–15].

Electromagnetic reactions can provide good constraints of the off-shell behavior of the potential. The potentials of category A have been tested at large on quite a number of observables in the photo- and electrodisintegration of the two-body system. The comparison with data is very good, at least within the nonrelativistic regime (see, e.g., Refs. [16,17]). As to category B potentials, analogous systematic studies are still missing. Investigations on electromagnetic reactions have been performed also in the three-body systems (see, e.g., Refs. [18–21]) for potentials falling into category A and B.

Due to its large binding energy the four-body system represents a very good testing ground for off-shell versus many-body properties of the nuclear force. However, an *ab initio* calculation of the total photodisintegration cross section of ^4He has been performed [22] with a category A potential of local nature (AV18 and UIX [5,8]) only recently. Even if the lack of precise experimental data limits the validity of such kind of calculations as test of the off-shell behavior of the potentials, it is interesting to calculate the same observable also with a potential of category C. In particular, one can ask whether potential models that reproduce the binding energy of the α particle in two different ways, either by including three-body operators or by a proper choice of the off-shell behavior of the two-body potential, predict the same results for the electromagnetic observables.

Among the potentials of category C, of particular interest are the potentials of Refs. [12–14], which are highly nonlocal and given in terms of matrix elements constructed by means

*On leave of absence from Department of Physics, University of Trento, I-38050 Povo (Trento), Italy.

of the J -matrix version of inverse scattering theory. Due to the lack of the three-body operator and the way they are constructed, they lead to rapid convergence, when used in many-body *ab initio* calculations based on complete basis expansions, as was shown in Ref. [13] within the no core shell-model approach [23].

The aim of this work is twofold. On the one hand we want to extend the calculation of Ref. [22] to nonlocal potentials. On the other hand we would like to compare the results on the total photodisintegration of ${}^2\text{H}$, ${}^3\text{H}$, and ${}^3,4\text{He}$ below pion threshold, obtained with two versions of the JISP, to those given by typical category A potentials.

We have chosen this particular electromagnetic observable because in this case the validity of Siegert's theorem allows to take largely into account, in an implicit way, the two- (or more-) body current contributions. Because of the particular form of the JISP (in matrix and not in operator form) it would be otherwise very difficult, if not impossible, to construct them in a consistent way. However, just these currents can help to get an idea on the importance of the underlying degrees of freedom that are "mocked" by the off-shell part of the potential.

The photodisintegration cross sections are calculated here using the Lorentz integral transform (LIT) method [24], which allows the treatment of the continuum states dynamics by means of a bound state technique. This method is briefly summarized in Sec. II. We use the symmetrized HH expansion [25–28] for the three- and four-body calculations, whereas standard numerical methods are used to solve the differential equations in the two-body case.

The use of the HH formalism is natural in configuration space and for local potentials. Because the JISP are nonlocal and given in terms of two-body matrix elements between harmonic oscillator (HO) states, the many-body HH formalism has to be adapted to this case. Section III contains the description of how this is achieved. In Sec. IV we present the results for the total photodisintegration of $A = 2, 3, 4$ nuclei and compare them to those obtained by category A potentials. Conclusions are drawn in Sec. V.

II. THE TOTAL PHOTOABSORPTION CROSS SECTION WITH THE LIT METHOD

The total photoabsorption cross section is given by

$$\sigma_\gamma(\omega) = 4\pi^2\alpha\omega R(\omega), \quad (1)$$

where α is the fine structure constant, ω represents the energy transferred by the photon, and $R(\omega)$ is the response function defined as

$$R(\omega) = \sum_f^{\downarrow} |\langle f | \Theta | 0 \rangle|^2 \delta(E_f - \omega - E_0). \quad (2)$$

Here $|0\rangle$ and E_0 are the nuclear ground-state wave function and energy, $|f\rangle$ and E_f denote eigenstates and eigenvalues of the nuclear Hamiltonian H , and Θ is the operator relevant to this reaction (it is assumed that recoil effects are negligible). In the low-energy region considered here one can rely on Siegert's

theorem and use for Θ the unretarded dipole operator

$$\Theta = \frac{1}{2} \sum_i^A z_i \tau_i^3. \quad (3)$$

The calculation of $R(\omega)$ seems to require the knowledge of the continuum states $|n\rangle$. However, this difficulty can be avoided using the LIT method. This method has been described extensively in several publications [24,29]. Here we summarize only the three steps that are needed for the calculation of $R(\omega)$.

Step 1. The equation

$$(H - E_0 - \omega_0 + i\Gamma)|\tilde{\Psi}\rangle = \Theta|0\rangle \quad (4)$$

has to be solved for many ω_0 and a fixed Γ . This is a Schrödinger-like equation with a source. It can be shown easily that the solution $|\tilde{\Psi}\rangle$ is localized. Thus one only needs a bound state technique to calculate it. One generally adopts the same bound state technique as for the solution of the ground state, which is an input for Eq. (4). We use expansions on the HH basis, as explained in Sec. III.

The values of the parameters ω_0 and Γ are chosen in relation to the physical problem. In fact, as it becomes clear in *Step 2*, the value of Γ is a kind of "energy resolution" for the response function and the values of ω_0 scan the region of interest. In our case we are interested in the resonance region and up to pion threshold. Therefore we solve Eq. (4) with $\Gamma = 10$ and 20 MeV and for a few hundred of ω_0 values chosen in the interval from -10 to 200 MeV.

Step 2. After solving Eq. (4) the overlap $\langle \tilde{\Psi} | \tilde{\Psi} \rangle$ is calculated. Of course this overlap depends on ω_0 and Γ . A theorem for integral transforms based on the closure property of the Hamiltonian eigenstates [30] ensures that this dependence can be expressed as [24]

$$L(\omega_0, \Gamma) = \langle \tilde{\Psi} | \tilde{\Psi} \rangle = \int R(\omega) \mathcal{L}(\omega, \omega_0, \Gamma) d\omega, \quad (5)$$

where \mathcal{L} is the Lorentzian function centered at ω_0 and with Γ as a width:

$$\mathcal{L}(\omega, \omega_0, \Gamma) = \frac{1}{(\omega - \omega_0)^2 + \Gamma^2}. \quad (6)$$

Therefore by solving Eq. (4) one can easily obtain the LIT of the response function.

Step 3. The transform (5) is inverted (see, e.g., Ref. [29, 31]) to obtain the response function and therefore the cross section. Of course the inversion result has to be independent of Γ and show a high degree of stability.

III. ACCOMMODATION OF NONLOCAL NN POTENTIAL MATRIX ELEMENTS IN THE HH FORMALISM

In this section we describe the implementation of nonlocal potentials in the HH formalism. Our method is alternative to that of Ref. [32] and more convenient for the structure of our codes.

A. The A -body basis states

In the HH formalism the antisymmetric A -body configuration-spin-isospin basis functions with total angular momentum J_A, J_A^z and isospin T_A, T_A^z are given by (notations as in Ref. [33])

$$\begin{aligned} & |n_A K_A J_A J_A^z T_A T_A^z \Gamma_A \alpha_A \beta_A\rangle \\ &= |n_A\rangle \sum_{Y_{A-1}} \frac{\Lambda_{\Gamma_A, Y_{A-1}}}{\sqrt{|\Gamma_{A-1}|}} [|K_A L_A M_A \Gamma_A Y_{A-1} \alpha_A\rangle \\ & \quad \times |S_A S_A^z T_A T_A^z \tilde{\Gamma}_A, \tilde{Y}_{A-1} \beta_A\rangle]_{J_A^z}^{J_A}, \end{aligned} \quad (7)$$

where

$$\langle \Omega_A | K_A L_A M_A \Gamma_A Y_{A-1} \alpha_A \rangle \equiv \mathcal{Y}_{K_A L_A M_A \Gamma_A Y_{A-1} \alpha_A}^{[A]}(\Omega_A) \quad (8)$$

are the HH functions with hyperspherical angular momentum K_A , and orbital angular momentum quantum numbers L_A, M_A that belong to well-defined irreducible representations (irreps) $\Gamma_1 \in \Gamma_2 \dots \in \Gamma_A$ of the permutation group-subgroup chain $\mathcal{S}_1 \subset \mathcal{S}_2 \dots \subset \mathcal{S}_A$, denoted by the Yamanouchi symbol $[\Gamma_A, Y_{A-1}] \equiv [\Gamma_A, \Gamma_{A-1}, \dots, \Gamma_1]$. The dimension of the irrep Γ_m is denoted by $|\Gamma_m|$ and $\Lambda_{\Gamma_A, Y_{A-1}}$ is a phase factor [34]. Similarly, the functions

$$\begin{aligned} & \langle s_1^z \dots s_A^z, t_1^z \dots t_A^z | S_A S_A^z T_A T_A^z \tilde{\Gamma}_A, \tilde{Y}_{A-1} \beta_A \rangle \\ & \equiv \chi_{S_A S_A^z T_A T_A^z \tilde{\Gamma}_A, \tilde{Y}_{A-1} \beta_A}^{[A]}(s_1^z \dots s_A^z, t_1^z \dots t_A^z) \end{aligned} \quad (9)$$

are the symmetrized spin-isospin basis functions. In Eqs. (8) and (9) the quantum numbers α_A, β_A are used to remove the degeneracy of the HH and spin-isospin states, respectively. The function

$$\langle \rho | n_A \rangle = R_{n_A}^{[A]}(\rho) \quad (10)$$

is the A -body hyperradial basis function,

$$\begin{aligned} R_{n_A}^{[A]}(\rho) &= \sqrt{\frac{n_A!}{(n_A + \alpha_L)!}} b^{-3(A-1)/2} \left(\frac{\rho}{b}\right)^{(\alpha_L - 3A + 4)/2} \\ & \quad \times L_{n_A}^{\alpha_L}(\rho/b) \exp[-\rho/(2b)], \end{aligned} \quad (11)$$

where $L_n^{\alpha}(x)$ are the associated Laguerre polynomials. The A -body hyperradial basis functions depend on the range parameter b and the Laguerre parameter α_L .

For the sake of brevity in the following the state of Eq. (7) will be denoted by $|n_A, [K_A]\rangle$, with $[K_A] \equiv K_A J_A J_A^z T_A T_A^z \Gamma_A \alpha_A \beta_A$.

B. The interaction and the HH ($A-2, 2$) basis

The representation of a non-local two-body interaction becomes very simple if the basis for the A -body Hilbert space is chosen as an outer product of a two-particle and a $(A-2)$ -particle states. In such a representation the interaction has the following form

$$v^{[2]}(ij) = \sum_{c_2 c_2'} |c_2 C_{A-2}\rangle v_{c_2 c_2'}^{[2]} \langle c_2' C_{A-2}|, \quad (12)$$

where by c_2 and c_2' we denote the two-body states of the interacting particles ij and by C_{A-2} we indicate a state that

includes the $(A-2)$ -body residual system. For a fermion system, these states should be taken as antisymmetric two-body and $(A-2)$ -body states, respectively.

We choose to label the particles of the pair as particle A and $A-1$ and to indicate their relative coordinate by $\vec{\eta} \equiv \vec{\eta}_{A-1} = \sqrt{\frac{1}{2}}(\vec{r}_A - \vec{r}_{A-1})$. Thus c_2 depends on the Jacobi coordinate $\vec{\eta}_{A-1}$ and C_{A-2} on the remaining $(A-2)$ reversed order Jacobi coordinates $\vec{\eta}_{A-2}, \vec{\eta}_{A-3}, \dots, \vec{\eta}_1$ [27]. Notice that in this way C_{A-2} has information also on the relative orientation of the two- and the $(A-2)$ -body subsystems.

After having transformed $\{\vec{\eta}_{A-2}, \vec{\eta}_{A-3}, \dots, \vec{\eta}_1\}$ and $\vec{\eta}$ to hyperspherical and spherical coordinates, respectively, one can express C_{A-2} (c_2) on the hyperspherical (spherical) basis. In analogy to Eq. (7) one has the antisymmetric $(A-2)$ -body configuration-spin-isospin states

$$\begin{aligned} |C_{A-2}\rangle &= |n_{A-2}\rangle \sum_{Y_{A-3}} \frac{\Lambda_{\Gamma_{A-2}, Y_{A-3}}}{\sqrt{|\Gamma_{A-2}|}} \\ & \quad \times [|K_{A-2} L_{A-2} M_{A-2} \Gamma_{A-2} Y_{A-3} \alpha_{A-2}\rangle \\ & \quad \times |S_{A-2} S_{A-2}^z T_{A-2} T_{A-2}^z \tilde{\Gamma}_{A-2}, \tilde{Y}_{A-3} \beta_{A-2}\rangle]_{J_{A-2}^z}^{J_{A-2}}, \end{aligned} \quad (13)$$

and the antisymmetric two-body states (the sum $\ell_2 + S_2 + T_2$ is odd)

$$|c_2\rangle = |n_2\rangle [|\ell_2 m_2\rangle |S_2 S_2^z T_2 T_2^z\rangle]_{J_2^z}^{J_2}. \quad (14)$$

The notations in the previous equations are similar to those in Eqs. (7) and (8). The difference is in the subscripts $A-2$ and 2 , indicating that the quantum numbers refer to the $(A-2)$ system and to the pair, respectively. Therefore the corresponding HH, spin-isospin and hyperradial functions are $\mathcal{Y}_{K_{A-2} L_{A-2} M_{A-2} \Gamma_{A-2} Y_{A-3} \alpha_{A-2}}^{[A-2]}(\Omega_{A-2})$ and $Y_{\ell_2 m_2}(\Omega_2 = \hat{\eta})$, $\chi_{S_{A-2} S_{A-2}^z T_{A-2} T_{A-2}^z \tilde{\Gamma}_{A-2}, \tilde{Y}_{A-3} \beta_{A-2}}^{[A-2]}(s_1^z \dots s_{A-2}^z, t_1^z \dots t_{A-2}^z)$ and $\chi_{S_2 S_2^z T_2 T_2^z}^{[2]}(s_1^z s_2^z, t_1^z t_2^z)$, $R_{n_{A-2}}^{[A-2]}(\rho_{A-2})$ and $R_{n_2}^{[2]}(\eta)$, respectively. Moreover, in the following $|C_{A-2}\rangle$ will be denoted by $|n_{A-2}, [K_{A-2}]\rangle$ and $|c_2\rangle$ by $|n_2, [K_2]\rangle$.

To calculate the matrix elements of the potential between the A -body states of Eq. (7), it is also useful to introduce a particular HH basis that reflects the division of the particle system into a pair of interacting particles and an $(A-2)$ spectator. Such a basis is obtained by coupling the two- and $(A-2)$ -body spherical-spin-isospin states and hyperspherical-spin-isospin states to yield an A -body basis function with quantum numbers $[K_{A-2}], [K_2], K_A, J_A, J_A^z, T_A, T_A^z$, through the relation

$$\begin{aligned} | [K_{A-2}]; [K_2] \rangle K_A J_A J_A^z T_A T_A^z &= \mathcal{N}_n^{a,b} (\sin \theta_{[A-2,2]})^{\ell_2} \\ & \quad \times (\cos \theta_{[A-2,2]})^{K_{A-2}} P_n^{(a,b)} \\ & \quad \times (\cos 2\theta_{[A-2,2]}) [|[K_{A-2}]\rangle] \\ & \quad \times |[[K_2]] \rangle_{J_A^z T_A^z}^{J_A T_A}, \end{aligned} \quad (15)$$

where $\theta_{[A-2,2]}$ is defined by the following equations

$$\begin{aligned} \eta &= \rho \sin \theta_{[A-2,2]} \\ \rho_{A-2} &= \rho \cos \theta_{[A-2,2]}. \end{aligned} \quad (16)$$

Here $P_n^{(a,b)}$ are the Jacobi polynomials, with arguments

$$\begin{aligned} a &= \ell_2 + 1/2 \\ b &= K_{A-2} + \frac{3A-8}{2} \\ n &= \frac{K_A - K_{A-2} - \ell_2}{2}. \end{aligned} \quad (17)$$

The numerical factor

$$\mathcal{N}_n^{a,b} = \sqrt{\frac{2(2n+a+b)n!\Gamma(n+a+b+1)}{\Gamma(n+a+1)\Gamma(n+b+1)}} \quad (18)$$

is a normalization constant.

For the sake of brevity we use the following notation:

$$P_{K_A}^{K_{A-2}, \ell_2} \equiv \mathcal{N}_n^{a,b} (\sin \theta_{[A-2,2]})^{\ell_2} (\cos \theta_{[A-2,2]})^{K_{A-2}} P_n^{(a,b)} \times (\cos 2\theta_{[A-2,2]}).$$

Therefore the HH $(A-2, 2)$ basis states $|[K_{A-2}]; [K_2]K_A J_A J_A^z T_A T_A^z\rangle$ can now be written as

$$\begin{aligned} |[K_{A-2}]; [K_2]K_A J_A J_A^z T_A T_A^z\rangle &= P_{K_A}^{K_{A-2}, \ell_2} |[K_{A-2}] \\ &\times |[K_2]\rangle_{J_A^z T_A^z}^{J_A T_A}. \end{aligned} \quad (19)$$

These states, together with the A -body hyperradial basis states $|n_A\rangle$, form a complete orthonormal basis of our Hilbert space.

C. The transformation between the A and $(A-2, 2)$ basis

The next step is the evaluation of the overlaps between the A -body functions, Eq. (7), and the $(A-2)$ - and two-body functions, Eqs. (13) and (14). To this end we use the completeness of the HH $(A-2, 2)$ basis, Eq. (19), i.e.,

$$\begin{aligned} \langle n_A, [K_A] | n_{A-2}, [K_{A-2}]; n_2, [K_2] \rangle &= \\ \sum \langle n_A, [K_A] | n_A, ([K_{A-2}]; [K_2]) K_A J_A J_A^z T_A T_A^z \rangle & \\ \times \langle n_A, ([K_{A-2}]; [K_2]) K_A J_A J_A^z T_A T_A^z | & \\ \times n_{A-2}, [K_{A-2}]; n_2, [K_2] \rangle. & \end{aligned} \quad (20)$$

Let us start with the first matrix element on the right-hand side of Eq. (20). The contributions of the hyperangular, spin, and isospin matrix elements are evaluated with the help of $6j$ and $9j$ symbols, the hyperspherical coefficients of fractional parentage (CFPs) and the spin-isospin CFPs [35]. One has

$$\begin{aligned} \langle [K_A] | ([K_{A-2}]; [K_2]) K_A J_A J_A^z T_A T_A^z \rangle &= \\ \times \sqrt{(2J_{A-2}+1)(2J_2+1)(2S_A+1)(2L_A+1)} & \\ \times \left\{ \begin{array}{ccc} S_2 & S_{A-2} & S_A \\ \ell_2 & L_{A-2} & L_A \\ J_2 & J_{A-2} & J_A \end{array} \right\} \sum_{\Gamma_{A-1}} \Lambda_{\Gamma_A, \Gamma_{A-1}} \Lambda_{\Gamma_{A-1}, \Gamma_{A-2}} \sqrt{\frac{|\Gamma_{A-2}|}{|\Gamma_A|}} & \\ \times \langle K_A L_A Y_A \alpha_A | (K_{A-2} L_{A-2} Y_{A-2} \alpha_{A-2}; \ell_2) K_A L_A \rangle & \\ \times \langle S_A T_A \tilde{Y}_A \beta_A | (S_{A-2} T_{A-2} \tilde{Y}_{A-2} \beta_{A-2}; S_2 T_2) S_A T_A \rangle, & \end{aligned} \quad (21)$$

where the hyperspherical matrix elements are written as

$$\begin{aligned} \langle K_A L_A Y_A \alpha_A | (K_{A-2} L_{A-2} Y_{A-2} \alpha_{A-2}; \ell_2) K_A L_A \rangle &= \\ \times \sum_{\alpha_{A-1}} \langle K_A L_A \Gamma_{A-1} \alpha_{A-1} | K_A L_A \Gamma_A \alpha_A \rangle & \\ \times \langle (K_{A-2} L_{A-2} \Gamma_{A-2} \alpha_{A-2}; \ell_2) K_A L_A | K_A L_A \Gamma_{A-1} \alpha_{A-1} \rangle & \end{aligned} \quad (22)$$

and, analogously, the spin-isospin term is written as

$$\begin{aligned} \langle S_A T_A \tilde{Y}_A \beta_A | (S_{A-2} T_{A-2} \tilde{Y}_{A-2} \beta_{A-2}; S_2 T_2) S_A T_A \rangle &= \\ \sum_{S_{A-1} T_{A-1} \beta_{A-1}} \Pi T S C F P_A \langle S_{A-2} S_{A-1} S_A | (S_{A-2}; S_2) S_A \rangle & \\ \times \langle T_{A-2} T_{A-1} T_A | (T_{A-2}; T_2) T_A \rangle, & \end{aligned} \quad (23)$$

with CFPs products

$$\begin{aligned} \Pi T S C F P_A &= \langle S_A S_{A-1} T_A T_{A-1} \tilde{\Gamma}_{A-1} \beta_{A-1} | S_A T_A \tilde{\Gamma}_A \beta_A \rangle \\ &\times \langle S_{A-1} S_{A-2} T_{A-1} T_{A-2} \tilde{\Gamma}_{A-2} \beta_{A-2} | \\ &\times S_{A-1} T_{A-1} \tilde{\Gamma}_{A-1} \beta_{A-1} \rangle. \end{aligned} \quad (24)$$

The spin-isospin matrix elements can be easily evaluated using angular momentum techniques:

$$\begin{aligned} \langle T_{A-2} T_{A-1} T_A | (T_{A-2}; T_2) T_A \rangle &= \\ (-)^{T_A+T_{A-2}+1} \sqrt{(2T_{A-1}+1)(2T_2+1)} \left\{ \begin{array}{ccc} T_{A-2} & t & T_{A-1} \\ t & T_A & T_2 \end{array} \right\}. & \end{aligned} \quad (25)$$

Here t is equal to $\frac{1}{2}$ and stands for the isospin of a single nucleon. The spin matrix element can be obtained by simply replacing in Eq. (25) the isospin quantum numbers by corresponding spin quantum numbers. The overlap between the interaction basis and the HH $(A-2, 2)$ states are given by

$$\begin{aligned} \langle n_A, ([K_{A-2}]; [K_2]) K_A J_A J_A^z T_A T_A^z | n_{A-2}, [K_{A-2}]; n_2, [K_2] \rangle &= \\ \langle J_{A-2} J_{A-2}^z J_2 J_2^z | J_A J_A^z \rangle \langle T_{A-2} T_{A-2}^z T_2 T_2^z | T_A T_A^z \rangle \Delta_{n_A}^{n_{A-2} n_2} & \\ \times (K_A, K_{A-2}, \ell_2), & \end{aligned} \quad (26)$$

where

$$\begin{aligned} \Delta_{n_A}^{n_{A-2} n_2} (K_A, K_{A-2}, \ell_2) &= \int \eta^2 d\eta R_{n_2 \ell_2}^{[2]}(\eta) \\ &\times \int \rho_{A-2}^{3A-7} d\rho_{A-2} R_{n_{A-2}}^{[A-2]}(\rho_{A-2}) \\ &\times R_{n_A}^{[A]}(\rho) P_{K_A}^{K_{A-2}, \ell_2}(\cos \theta_{[A-2,2]}). \end{aligned} \quad (27)$$

This two-dimensional integral can be easily evaluated using the Gauss-quadrature integration.

D. The potential matrix elements

Using the representation of the potential as in Eq. (12) and the overlaps $\langle n_A, [K_A] | c_2 C_{A-2} \rangle$ calculated above, the A -body matrix elements of a scalar-isoscalar two-body operator can be written as

$$\begin{aligned} \langle n_A [K_A] | v^{[2]}(A, A-1) | n'_A [K'_A] \rangle &= \\ \sum_{c_2 c'_2 C_{A-2}} \langle n_A [K_A] | c_2 C_{A-2} \rangle v_{c_2 c'_2}^{[2]} \langle c'_2 C_{A-2} | n'_A [K'_A] \rangle &= \\ \sum_{[K_2], [K'_2], [K_{A-2}]} \sum_{[n_2], [n'_2], [n_{A-2}]} \Delta_{n_A}^{n_{A-2} n'_2} (K_A, K_{A-2}, \ell_2) \Delta_{n'_A}^{n_{A-2} n'_2} & \\ \times \langle K'_A, K_{A-2}, \ell'_2 \rangle \langle [K_A] | (K_{A-2}); [K_2] \rangle K_A J_A J_A^z T_A T_A^z & \\ \times \langle [K'_A] | (K_{A-2}); [K'_2] \rangle K'_A J_A J_A^z T_A T_A^z & \\ \times v_{n_2 [K_2], n'_2 [K'_2]}^{[2]}(A, A-1), & \end{aligned} \quad (28)$$

where we have used the orthogonality of the Clebsch Gordon coefficients

$$\sum_{J_2^z J_{A-2}^z} \langle J_{A-2} J_{A-2}^z J_2 J_2^z | J_A J_A^z \rangle \langle J_{A-2} J_{A-2}^z J_2 J_2^z | J'_A J_A^z \rangle = \delta_{J_A J'_A} \delta_{J_A^z J_A^z} \quad (29)$$

and

$$\sum_{T_2^z T_{A-2}^z} \langle T_{A-2} T_{A-2}^z T_2 T_2^z | T_A T_A^z \rangle \langle T_{A-2} T_{A-2}^z T_2 T_2^z | T'_A T_A^z \rangle = \delta_{T_A T'_A} \delta_{T_A^z T_A^z}. \quad (30)$$

Finally, the actual potential matrix elements are calculated via

$$v_{n_2[K_2], n_2'[K_2']}^{[2]} = \delta_{J_2 J_2'} \delta_{J_2^z J_2'^z} \delta_{T_2 T_2'} \delta_{T_2^z T_2'^z} \langle n_2 \ell_2 S_2 J_2 J_2^z T_2 T_2^z | v^{[2]} | n_2' \ell_2' S_2' J_2' J_2'^z T_2' T_2'^z \rangle. \quad (31)$$

E. Application to the J -matrix inverse scattering potentials

In view of the use of the JISP as given in Ref. [12,14], a convenient choice for the configuration space two-body basis functions are the HO states,

$$(\vec{r} | n_2 \ell_2 m_2 \rangle_{HO} = R_{n_2 \ell_2}^{HO}(r) Y_{\ell_2 m_2}(\hat{r}), \quad (32)$$

with the radial function

$$R_{n_2 \ell_2}^{HO}(r) = \frac{(-1)^{n_2}}{r} \sqrt{\frac{2n!}{r_0 \Gamma(n + l + 3/2)}} \left(\frac{r}{r_0}\right)^{\ell_2+1} \times \exp[-r^2/(2r_0^2)] L_{n_2}^{\ell_2+\frac{1}{2}}(r^2/r_0^2). \quad (33)$$

Here r is the distance between the two particles, i.e., $r \equiv |\vec{r}_1 - \vec{r}_2|$, r_0 is related to the oscillator strength Ω_{HO} and the reduced mass μ through the relation $r_0 = \sqrt{\hbar/\mu\Omega_{HO}}$. However, the basis states in Eq. (32) do not possess the proper normalization. In fact they are normalized according to

$$\int d\vec{r} |\langle \vec{r} | nlm \rangle_{HO}|^2 = 1, \quad (34)$$

whereas in the canonical transformation from the single-particle coordinates to the center of mass and reversed order Jacobi coordinates the appropriate normalization is

$$\int d\vec{\eta} |\langle \vec{\eta} | nlm \rangle|^2 = 1, \quad (35)$$

where $\vec{\eta} = \sqrt{\frac{1}{2}}(\vec{r}_A - \vec{r}_{A-1}) = \sqrt{\frac{1}{2}}\vec{r}$. Consequently a normalization factor of $\sqrt[4]{8}$ has to be introduced. Therefore the appropriate two-body basis functions are

$$\begin{aligned} \langle \vec{\eta} | n_2 \ell_2 m_2 \rangle &= R_{n_2 \ell_2}^{[2]}(\eta) Y_{\ell_2 m_2}(\hat{\eta}) \\ &= \sqrt[4]{8} R_{n_2 \ell_2}^{HO}(r = \sqrt{2}\eta) Y_{\ell_2 m_2}(\hat{\eta}). \end{aligned} \quad (36)$$

TABLE I. Binding energies [MeV] for $A = 3, 4$ nuclei using the HH expansion with the JISP6 and JISP16 potentials. For comparison we also present the results obtained in the NCSM approach.

Nucleus	JISP6		JISP16	
	HH	NCSM [12]	HH	NCSM [14]
^3H	8.461(1)	8.461(5)	8.369(1)	8.354
^3He	7.749(1)	7.751(3)	7.662(1)	7.648
^4He	28.602(1)	28.611(41)	28.299(1)	28.297

IV. RESULTS

In the following we discuss the results for the unretarded total photoabsorption cross section of the two-, three-, and four-nucleon systems obtained with the JISP and compare them to the results given by other nuclear force models. For the three- and four-body systems the cross sections are calculated with the LIT method, as outlined in Sec. II, and using HH expansions of ground-state wave function and Ψ . For the JISP these HH expansions have rather rapid convergences, though no effective interaction has been introduced in this case. We obtain convergent binding energies of the three- and four-body systems with $K \leq 20$ (see Table I), whereas for potentials such as AV18 one needs K larger than 100. For the deuteron photoabsorption with the JISP we also use the LIT method but here combined with expansions on HO functions. For the other NN potentials a conventional calculation with explicit NN final-state wave functions is carried out (for one of these potentials it was checked that we get the same result also with the LIT method).

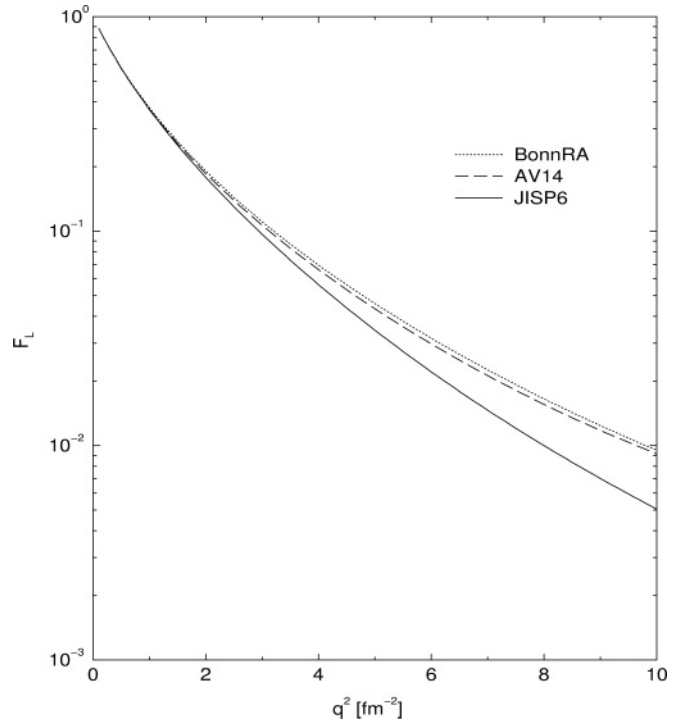


FIG. 1. Deuteron elastic longitudinal form factor (see text) for three different potential models.

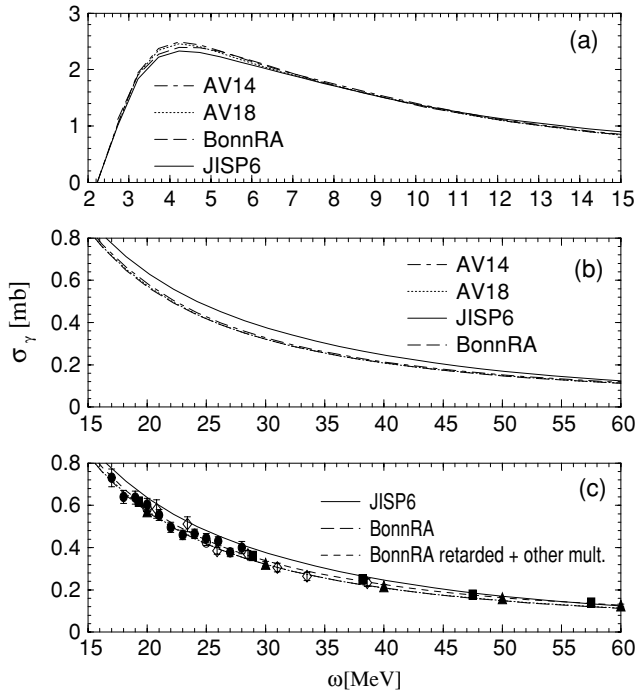


FIG. 2. Deuteron total photoabsorption cross section at lower (a) and higher (b) photon energies for four different potential models. Comparison with data for two potentials (see text) is shown in (c): open circles [38], solid squares [42], open diamonds [40], solid triangles [41], solid circles [39].

Before discussing the total photoabsorption cross sections we first consider the longitudinal deuteron elastic form factor $F_L(q^2)$. In Fig. 1 we show results for the JISP6 [12], AV14 [4], and BonnRA [1] potential models (note that the proton and neutron electric form factors are set equal to 1 and 0, respectively). Up to a momentum transfer $q^2 = 2 \text{ fm}^{-2}$ all models lead to rather similar results, whereas for higher q^2 the JISP6 result is considerably lower than those of the other two potential models. In comparison with experimental data one usually considers the elastic deuteron form factors $A(q^2)$ and $B(q^2)$, where $A(q^2)$ contains in addition to the longitudinal also a transverse contribution. However, in the momentum range shown in Fig. 1 the transverse piece is very small (see, e.g., Ref. [36]). For this momentum range it is known that the $A(q^2)$ of conventional potential models like AV14 or BonnRA agree well with experimental data (see, e.g., Ref. [4]). Thus one may conclude that the JISP6 potential leads to a good description of data only up to $q^2 = 2 \text{ fm}^{-2}$. However, this might be sufficient for the calculation of electromagnetic low-momentum transfer reactions such as nuclear photoabsorption below pion threshold.

In Fig. 2 the unretarded deuteron total photoabsorption cross section is shown for various potential models. In Fig. 2(a) one sees that the low-energy peaks have slightly different heights (note that the cross section below about 5 MeV is also affected by the here not considered M1 contribution). Beyond the peak one finds a good agreement of all models up to about 10 MeV. At higher photon energies one has very similar results for the AV14, AV18 [5], BonnRA models, whereas the

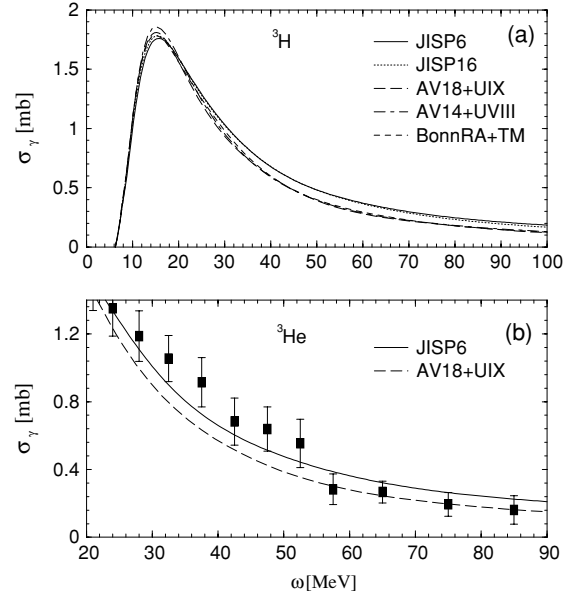


FIG. 3. Three-body total photoabsorption cross sections: (a) ${}^3\text{H}$ results for five different potential models; (b) ${}^3\text{He}$ results for two potential models, compared to data from Ref. [44].

JISP6 result shows a somewhat higher cross section between 15 and 60 MeV [see Fig. 2(b)]. Figure 2(c) helps to understand the situation better. For the BonnRA potential we illustrate the effect of the inclusion of retardation and of other multipoles (electric and magnetic ones up to multipole order $L = 4$), where the nonrelativistic one-body current and the Siegert operator are considered (calculation corresponds to Arenhövel's *normal* calculation for the deuteron photodisintegration, see, e.g., Ref. [37]). One notes that the additional contributions increase the cross section only slightly. In principle one has to include also other current contributions (meson exchange, isobar, and relativistic currents); however, as shown in Fig. 7.1.8 of Ref. [37] these effects are rather small. In the considered energy range they lead to a reduction of the *normal* cross section between 2 and 3%, thus bringing the total result very close to the unretarded total photoabsorption cross section. In comparison to experimental data [38–42] there is good agreement of the unretarded cross section with the BonnRA potential, whereas with the JISP6 potential the data are somewhat overestimated.

Now we turn to the total photoabsorption cross section of ${}^3\text{H}$ and ${}^4\text{He}$. In Fig. 3(a) we show the triton case with the JISP6 and JISP16 potentials and for the nuclear force models AV14 [4] and UVIII [7]; AV18 [5] and UIX [8]; BonnRA [1] and Tucson-Melbourne (TM) [6]. Results for the AV14+UVIII and BonnRA+TM potentials are taken from Ref. [43]. The situation is similar to the deuteron case of Fig. 2: small differences among the low-energy peak heights of all potential models and beyond 20 MeV differences between the conventional nuclear force models and the JISP, which, however, are considerably more pronounced than for the deuteron case. Because beyond the peak there are no triton total photoabsorption cross section data available, the comparison with data is done for the ${}^3\text{He}$ case [see Fig. 3(b)], choosing

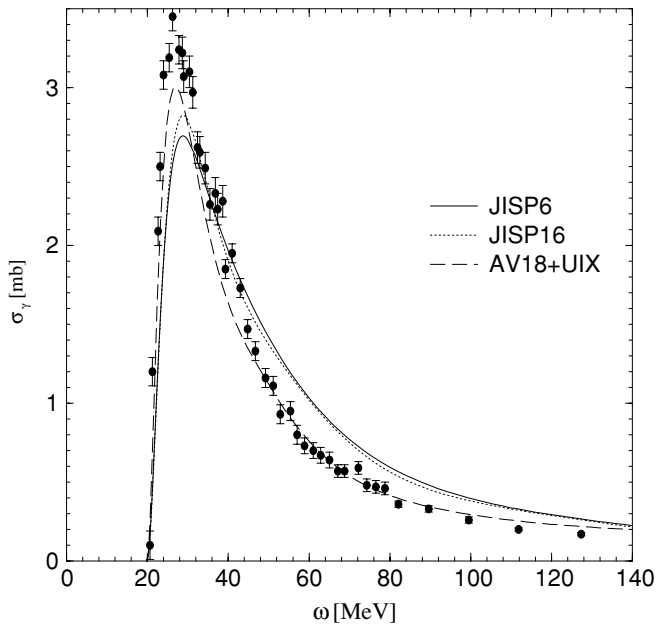


FIG. 4. Total photoabsorption cross section of ${}^4\text{He}$ for three different potential models. Experimental data from Ref. [45].

one of the JISP (JISP6) and one conventional (AV18+UIX) potential model. Unfortunately the data [44] have rather large error bars and do not lead to a clear picture. However, one can say that between 20 and 50 MeV there is a better agreement with the JISP6, whereas beyond 50 MeV the conventional potential models are favored.

In Fig. 4 we show the ${}^4\text{He}$ total photoabsorption cross section for the JISP6 and JISP16 potential models, as well as for the AV18+UIX nuclear force. The calculation for AV18+UIX is described in Ref. [22]. There it is discussed that the convergence of the HH expansion is rather slow because of the three-nucleon force. As already mentioned, for the JISP we find a much better convergence, though no effective interaction is introduced. In Fig. 4 one notices that the trend observed for deuteron and three-nucleon cases is confirmed. Beyond the peak the cross sections obtained with the JISP are considerably higher than that obtained using the conventional nuclear force model AV18+UIX. This effect is more pronounced than for the three-nucleon case, which in turn is already stronger than found for the deuteron case. In addition, for ${}^4\text{He}$ the JISP lead to somewhat lower peak heights and to a shift of the peak position by about 2 MeV toward higher energy, when compared to the AV18+UIX result. It is evident that the latter agrees much better with the experimental data [45]. Here we

should mention that the experimental situation is not yet settled (see also Ref. [22]), particularly regarding the height of the low-energy peak (the shown data are the only experimental total ${}^4\text{He}$ $\sigma_\gamma(\omega)$ results that extend to energies beyond the peak region).

V. CONCLUSIONS

In this work we have presented results for the total photoabsorption cross section of the two-, three-, and four-nucleon systems, obtained within the recently proposed J -matrix inverse scattering potential models.

The calculation in the three- and four-body systems are performed via the LIT method and the HH technique. To this aim the HH formalism has been adapted to accommodate nonlocal potentials.

The comparison of the JISP results with those obtained with a few more traditional realistic potentials, including two- and three-body forces, has shown that, whereas the latter give very similar results, JISP display a rather different behavior, especially beyond the resonance peak. The differences increase with the nuclear mass.

These results show that a “classical” electromagnetic observable as the total photonuclear cross section is able to emphasize the rather different off-shell properties of these two classes of potentials. In particular, in this observable nonlocalities of the two-body potential and three-body forces are not equivalent. Considering that, different from the JISP, the traditional potentials have in common the long-range one-pion exchange part, one may ascribe the discrepancies to this fact.

In the case of deuteron the comparison with data speaks in favor of the more traditional two-body potentials. For the three-body systems data are missing or have insufficient accuracy, making the comparison inconclusive. Regarding the four-body system the old data of Ref. [45] seem to favor the traditional potentials, as in the deuteron case. More recent data obtained in Lund [46], whereas measuring only the ${}^4\text{He}(\gamma, n)$ cross section point in this direction as well, provided that they are extrapolated to σ_γ by means of the charge symmetry argument.

More data of higher accuracy are very much needed to further clarify the issue of two- and three-body forces.

ACKNOWLEDGMENTS

We thank A. M. Shirokov for sending us the potential matrix elements of the JISP models. The work of N.B. was supported by the Israel Science Foundation (grant 361/05).

- [1] R. Machleidt, *Adv. Nucl. Phys.* **19**, 189 (1989).
- [2] R. Machleidt, *Phys. Rev. C* **63**, 24001 (2001).
- [3] V. G. J. Stoks, R. A. M. Klomp, C. P. F. Terheggen, and J. J. de Swart, *Phys. Rev. C* **49**, 2950 (1994).
- [4] R. B. Wiringa, R. A. Smith, and T. L. Ainsworth, *Phys. Rev. C* **29**, 1207 (1984).

- [5] R. B. Wiringa, V. G. J. Stoks, and R. Schiavilla, *Phys. Rev. C* **51**, 38 (1995).
- [6] S. A. Coon, M. D. Scadron, P. C. McNamee, B. R. Barrett, D. W. E. Blatt, and B. H. J. McKellar, *Nucl. Phys.* **A317**, 242 (1979); D. Hüber, J. L. Friar, A. Nogga, H. Witala, and U. van Kolck, *Few-Body Systems* **30**, 2001 (1995); J. L. Friar, D. Hüber, and U. van Kolck, *Phys. Rev. C* **59**, 53 (1999).

- [7] J. Carlson, V. R. Pandharipande, and R. B. Wiringa, Nucl. Phys. **A401**, 59 (1983).
- [8] B. S. Pudliner, V. R. Pandharipande, J. Carlson, S. C. Pieper, and R. B. Wiringa, Phys. Rev. C **56**, 1720 (1997).
- [9] S. C. Pieper, V. R. Pandharipande, R. B. Wiringa, and J. Carlson, Phys. Rev. C **64**, 014001 (2001).
- [10] S. R. Beane, P. F. Bedaque, W. C. Haxton, D. R. Phillips, and M. J. Savage, in *At the Frontier of Particle Physics*, edited by M. Shifman (World Scientific, Singapore, 2001); E. Epelbaum, A. Nogga, W. Glöckle, H. Kamada, Ulf.-G. Meissner, and H. Witala, Phys. Rev. C **66**, 064001 (2002); D. R. Entem and R. Machleidt, Phys. Lett. **B524**, 93 (2002); Phys. Rev. C **68**, 041001(R) (2003).
- [11] P. Doleschall, I. Borbély, Z. Papp, and W. Plessas, Phys. Rev. C **67**, 064005 (2003); P. Doleschall, Phys. Rev. C **69**, 054001 (2004).
- [12] A. M. Shirokov, J. P. Vary, A. I. Mazur, S. A. Zaytsev, and T. A. Weber, Phys. Lett. **B68**, 041001(R) (2003).
- [13] A. M. Shirokov, A. I. Mazur, S. A. Zaytsev, J. P. Vary, and T. A. Weber, Phys. Rev. C **70**, 044005 (2004).
- [14] J. A. M. Shirokov, J. P. Vary, A. I. Mazur, and T. A. Weber, ArXiv.org:nucl-th/0512105.
- [15] R. Roth, T. Neff, H. Hergert, and H. Feldmeier, Nucl. Phys. **A745**, 3 (2004).
- [16] K.-M. Schmitt and H. Arenhövel, Few-Body Syst. **11**, 33 (1991).
- [17] H. Arenhövel, W. Leidemann, and E. L. Tomusiak, Eur. Phys. J. A **23**, 147 (2005).
- [18] V. D. Efros, W. Leidemann, G. Orlandini, and E. L. Tomusiak, Phys. Lett. **B484**, 223 (2000).
- [19] J. Golak, R. Skibinski, W. Glöckle, H. Kamada, A. Nogga, H. Witala, V. D. Efros, W. Leidemann, G. Orlandini, and E. L. Tomusiak, Nucl. Phys. **A707**, 365 (2002).
- [20] R. Skibinski, J. Golak, H. Witala, W. Glöckle, H. Kamada, and A. Nogga, Phys. Rev. C **67**, 054002 (2003).
- [21] R. Skibinski, J. Golak, H. Witala, W. Glöckle, A. Nogga, and E. Epelbaum, ArXiv.org:nucl-th/0606021.
- [22] D. Gazit, S. Bacca, N. Barnea, W. Leidemann, and G. Orlandini, Phys. Rev. Lett. **96**, 112301 (2006).
- [23] D. C. Zheng, J. P. Vary, and B. R. Barrett, Phys. Rev. C **50**, 2841 (1994); D. C. Zheng, J. P. Vary, W. C. Haxton, and C. L. Song, Phys. Rev. C **52**, 2488 (1995); P. Navratil, J. P. Vary, and B. R. Barrett, Phys. Rev. Lett. **84**, 5728 (2000); Phys. Rev. C **62**, 054311 (2000).
- [24] V. D. Efros, W. Leidemann, and G. Orlandini, Phys. Lett. **B338**, 130 (1994).
- [25] N. Barnea and A. Novoselsky, Ann. Phys. (NY) **256**, 192 (1997).
- [26] N. Barnea and A. Novoselsky, Phys. Rev. A **57**, 48 (1998).
- [27] N. Barnea, Phys. Rev. A **59**, 1135 (1999).
- [28] A. Novoselsky and J. Katriel, Phys. Rev. A **49**, 833 (1994).
- [29] V. D. Efros, W. Leidemann, and G. Orlandini, Few-Body Syst. **26**, 251 (1999).
- [30] V. D. Efros, Yad. Fiz. **41**, 1498 (1985) [Sov. J. Nucl. Phys. **41**, 949 (1985)].
- [31] D. Andreasi, W. Leidemann, C. Reiss, and M. Schwamb, Eur. Phys. J. A **24**, 361 (2005).
- [32] M. Viviani, L. E. Marcucci, S. Rosati, A. Kievsky, and L. Girlanda, ArXiv.org:nucl-th/0512077.
- [33] N. Barnea, W. Leidemann, and G. Orlandini, Phys. Rev. C **67**, 054003 (2003).
- [34] A. Novoselsky, J. Katriel, and R. Gilmore, J. Math. Phys. **29**, 1368 (1988).
- [35] N. Barnea, W. Leidemann, and G. Orlandini, Nucl. Phys. **A650**, 427 (1999).
- [36] S. Galster *et al.*, Nucl. Phys. **B32**, 221 (1971).
- [37] H. Arenhövel and M. Sanzone, Few-Body Syst. Suppl. **3**, 1 (1991).
- [38] J. Ahrens, H. B. Eppler, H. Gimm, M. Kröning, P. Riehn, H. Wäffler, A. Zieger, and B. Ziegler, Phys. Lett. **B52**, 49 (1974).
- [39] D. M. Skopik, Y. M. Shin, M. C. Phenneger, and J. J. Murphy, Phys. Rev. C **9**, 531 (1974).
- [40] M. Bosman, A. Bol, J. F. Gilot, P. Leleux, P. Lipnik, and P. Macq, Phys. Lett. **B82**, 212 (1979).
- [41] M. P. De Pascale *et al.*, Phys. Lett. **B119**, 30 (1982).
- [42] R. Bernabei *et al.*, Phys. Rev. Lett. **57**, 1542 (1986).
- [43] V. D. Efros, W. Leidemann, G. Orlandini, and E. L. Tomusiak, Phys. Lett. **B484**, 223 (2000).
- [44] V. N. Fetisov, A. N. Gorbunov, and A. T. Varfolomeev, Nucl. Phys. **A71**, 305 (1965).
- [45] Yu. M. Arkatov *et al.*, Yad. Konst. **4**, 55 (1979).
- [46] B. Nilsson *et al.*, Phys. Lett. **B626**, 65 (2005).